# AB INITIO CALCULATIONS TARGETING CHEMICALLY ACCURATE THERMOCHEMICAL PROPERTIES OF ACTINIDE MOLECULES

By

ASHLEY R.E. HUNT

A thesis submitted in partial fulfillment of
the requirements for the degree of

MASTER OF SCIENCE IN CHEMISTRY

WASHINGTON STATE UNIVERSITY
Department of Chemistry

MAY 2023

To the Faculty of Washington State University:

The members of the Committee appointed to examine the thesis of ASHLEY R.E. HUNT find it satisfactory and recommend that it be accepted.

_____
Kirk A. Peterson, Ph.D., Chair

_____
James M. Boncella, Ph.D.

_____
David Feller, Ph.D.

_____
Xiaofeng Guo, Ph.D.

ACKNOWLEDGMENT

The author gratefully acknowledges the financial support from the U.S. Department of Energy, Office of Basic Energy Sciences, Heavy Element Chemistry program grant no. DE-SC0008501.

AB INITIO CALCULATIONS TARGETING CHEMICALLY ACCURATE THERMOCHEMICAL PROPERTIES OF ACTINIDE MOLECULES


Abstract

by Ashley R.E. Hunt, M.S.
Washington State University
May 2023

Chair: Kirk A. Peterson

Actinide molecules are fascinating to study, from their intrinsic role in nuclear energy to their significant relativistic effects. Computational efforts allow these molecules to be explored accurately with significantly fewer risks. Composite methods, such as the Feller-Peterson-Dixon (FPD) method, have had good success previously with accurately determining thermochemical properties of small actinide molecules. Here, FPD is used to explore the electron affinities of ThO and ThPt via the similar orbital character between O and Pt; the electron affinities of ThPtC as well as determine its appropriate ground state structure; and electron affinities, ionization potentials, and bond dissociation energies of uranium oxides and neptunium oxides. The values found were in excellent agreement with experimental measurements, if applicable, so long as the wavefunction could be adequately described as a single determinant. The bonding character of molecules of interest are also analyzed in this work.

TABLE OF CONTENTS

Page

LIST OF TABLES

Page

LIST OF FIGURES

Page

LIST OF EQUATIONS

Page

## Dedication

To John and Adeline Hunt, the two greatest gifts God has given me.

# CHAPTER ONE: INTRODUCTION

Small actinide species have been of great interest for decades. With their relativistic effects and large electron count, their unique chemistry is exciting to explore. Actinides often appear in relation to nuclear energy, such as thorium based molten salt reactors and uranium fuels with minor actinides like neptunium present via irradiation.[1–4] Some of these actinides are vaporized in the nuclear fuel cycle, such as in the enrichment stage.[4] To better serve nuclear fuel and related areas, fundamental knowledge of gas-phase actinide properties must be explored accurately. Actinide-containing molecules are not a new phenomenon but have been explored for decades. Relativistic effects, high electron count, and the introduction of the 5f orbitals make the study of actinide chemistry challenging, but also intriguing.[5]

Heavy relativistic effects cannot be ignored for actinides. For example, the positron solution of the wavefunction for the uranium 1s electron is about 25% the total size of the wavefunction.[6] The high electron count adds complexity to molecular orbitals and bonding interactions. The 5f orbitals appear to participate more heavily in covalent bonding than 4f orbitals.[7–11] The 5f orbitals also have a wider range of oxidation states[7,12–15]; for example, cerium has one of the highest oxidation states of a lanthanide (+4)[12] while uranyl ($UO_2^{2+}$) touts a +6 oxidation state.

Bonds between actinides and main group elements are well documented. Thorium creates strong bonds with elements like oxygen[16–19] and carbon.[16,20] Uranium has been found to bind with elements like boron[21], carbon[22], oxygen[23–27], and halides.[4] Transuranic elements, like plutonium, can bind with oxygen[3,4,28–34] and halides.[4,35] These can be larger molecules (U and Th complex references) or diatomic.

Actinide experiments are filled with challenges, as actinides are notoriously difficult to handle.[2] Computational methods can produce accurate values, such as thermochemical properties and geometries, with significantly fewer risks.[5] But performing a single calculation with a goal of obtaining chemical accuracy (1 kcal/mol) for a thermochemical property is not feasible for actinide systems. A composite approach that recognizes and accommodates for the different sources of error while still maintaining high accuracy is much more practical.

The ab initio Feller-Peterson-Dixon (FPD) composite method was used in this work to predict accurate thermochemical properties. This composite approach has had great success in predicting these properties throughout the periodic table.[27,36–40] It also includes relativistic modifications of the original methodology[37] to better tackle difficulties found in actinide systems. While this approach has been tested successfully in many areas, including with actinide ionization potentials (IPs)[19,22,40–42] and actinide bond dissociation energies (BDEs)[19,41–46] there are still many areas where it has been used infrequently, such as metalloactinyl thermochemical properties and electron affinities.[21,22,27,47] Therefore, this thesis seeks to address the application of the FPD procedure to small molecule systems via ab initio calculations in order to assess their thermochemical properties and structures.

In the case of ThO, the principle of isolobality, which states fragments are isolobal "if the number, symmetry properties, approximate energy and shape of the frontier orbitals and the number of electrons in them are similar"[48] can be applied to the relationship between O and Pt.[49] This provides a launching point for studying actinide-transition metal (An-TM) bonding. The bonding has been explored computationally by Feng et al.[27] regarding later actinide containing species (U, Np, and Pu). While experimental work has explored larger molecules containing a

thorium-TM bond[50–52] there does not appear to be a wide computational exploration into these species.

Actinide oxides have been studied extensively by both experiment and theory.[19,24–26,53–57] One recent computational study[5] involved characterizing ionization potentials for actinide (U-Cm) mono- and di-oxides computationally via CASSCF/CASPT2. There is interest in seeing if higher accuracy methods could provide greater accuracy to these findings. For example, higher accuracy methods could characterize specific features of these systems, such as spin-orbit coupling, which plays a large role in actinide containing molecules. A composite procedure, like FPD, can show these by design. By looking at other properties, such as electron affinities and bond dissociation energies, with the same composite method can potentially clarify what types of interactions, such as spin-orbit or core-valence orbital participation in bonding, are important in various types of reactions.

This thesis seeks to explore the structures and thermochemical properties of a variety of small actinide-containing molecules via the relativistic Feller-Peterson-Dixon (FPD) procedure, which will be explained in Chapter 2, in addition to the various theories, basis sets, and concepts used to correctly carry out an FPD calculation. Chapter 2 will also cover how this thesis plans to analyze bonding. Chapter 3 will look at ThO, a well-studied system, its electron affinity, and its correlation to unstudied ThPt via isolobality. Chapter 4 will build off these findings by discussing joint work with Dr. Bowen's at Johns Hopkins University, where an anion photoelectron spectrum is analyzed for the ground state structure of ThPtC- and further analyzation of metalloactinyl bonding. Chapter 5 will look at various thermochemical properties,

structures, and bond analyses of uranium and neptunium oxides, where the appropriateness of FPD method will be discussed. Chapter 6 will summarize the findings of this thesis.

# CHAPTER TWO: FELLER-PETERSON-DIXON METHOD

Quantum mechanically, the target level of theory is an exact solution of the Dirac-Coulomb-Breit Hamiltonian with perhaps some attention to quantum electrodynamic effects. However, this is not remotely possible for molecular systems, and hence a composite procedure is the only practical way to calculate quantities such as thermochemical properties of that can approach this level of accuracy. This allows various basis sets and levels of theory to be implemented, as any multi-electron system cannot be solved exactly, while taking appropriate, but necessary, approximations of both the Hamiltonian and the wavefunction. A good composite procedure maximizes accuracy without accruing unmanageable expense. For these calculations, each additional contribution is only included if the error of not including it is significant enough to not meet the targeted accuracy, e.g., 1 kcal/mol.[37,58,59] The flexibility of the Feller-Peterson-Dixon (FPD) methodology[37] makes it an excellent choice. The FPD procedure as used in this work can be summarized in Equation 2.1.[27,37]

$$E_{FPD} = E_{VQZ} + \Delta E_{CBS} + \Delta E_{CV} + \Delta E_{SO} + \Delta E_{Gaunt} + \Delta E_{QED} + E_{ZPE} \quad (2.1)$$

Here, $E_{FPD}$ is the total composite energy of the desired thermochemical property to be calculated. $E_{VQZ}$ is the base energy on which the remaining contributions are built. Unless otherwise specified, this uses an optimized frozen core (FC) coupled cluster singles and doubles with perturbative triples (CCSD(T))[60,61] geometry with valence quadruple zeta (QZ) basis sets. $\Delta E_{CBS}$ is the difference between the CCSD(T)/VQZ result and the complete basis set (CBS) limit.[6] $\Delta E_{CV}$ is the contribution associated with outer-core correlation; that is, the difference between CCSD(T)/CBS with valence and outer-core correlated and CCSD(T)/CBS with only valence electrons correlated. For actinide atoms the valence electrons include the 7s, 6d, 5f, 6p, and 6s

electrons while the outer core corresponds to the 5s, 5p, and 5d electrons. Weighted core valence basis sets, e.g., cc-pwCVnZ-X2C (n=T, Q), are used for this contribution. The cc-p(w)VnZ-X2C basis sets are designed to systematically converge to the CBS limit, at which the one-electron error introduced with the use of finite basis sets is eliminated. This can be estimated by extrapolating the energy using nZ and (n+1)Z basis sets via the Karton-Martin formula[27,62] (Equation 2.2) for the HF energy and Martin's formula[27,63,64] (Equation 2.3) for the correlation energy. Generally, n=3 has been used in this work, and $\alpha = 6.57$ when n, n+1 = 3,4. These preceding three calculations are all performed with MOLPRO.[65–67]

$$E_n = E_{CBS} + A(n+1)e^{-\alpha\sqrt{n}} \tag{2.2}$$

$$E_n = E_{CBS} + \frac{A}{(n+\frac{1}{2})^4} \tag{2.3}$$

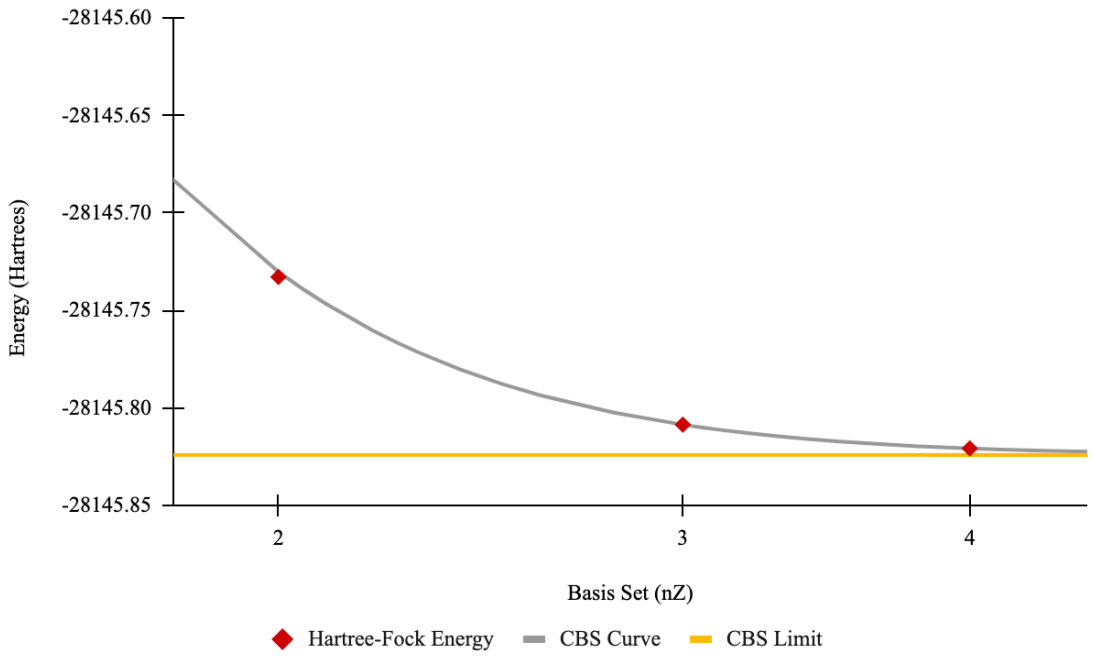


**Figure 2.1 – Systematic Convergence to the CBS Limit for the Hartree Fock Energy of $UO_2$**

For an example of how these basis sets converge to the CBS limit, $UO_2$ was calculated with augmented correlation consistent polarized valence n-zeta basis sets, aug-cc-pVnZ-X2C for O and cc-pVnZ-X2C for U, where n varied from 2 to 4.[68,69] The systematic decrease towards the CBS limit for the HF energy (Figure 2.1) and correlation energy (Figure 2.2) as the cardinal number of the basis set is increased shows how these basis sets are designed for this systematic convergence.

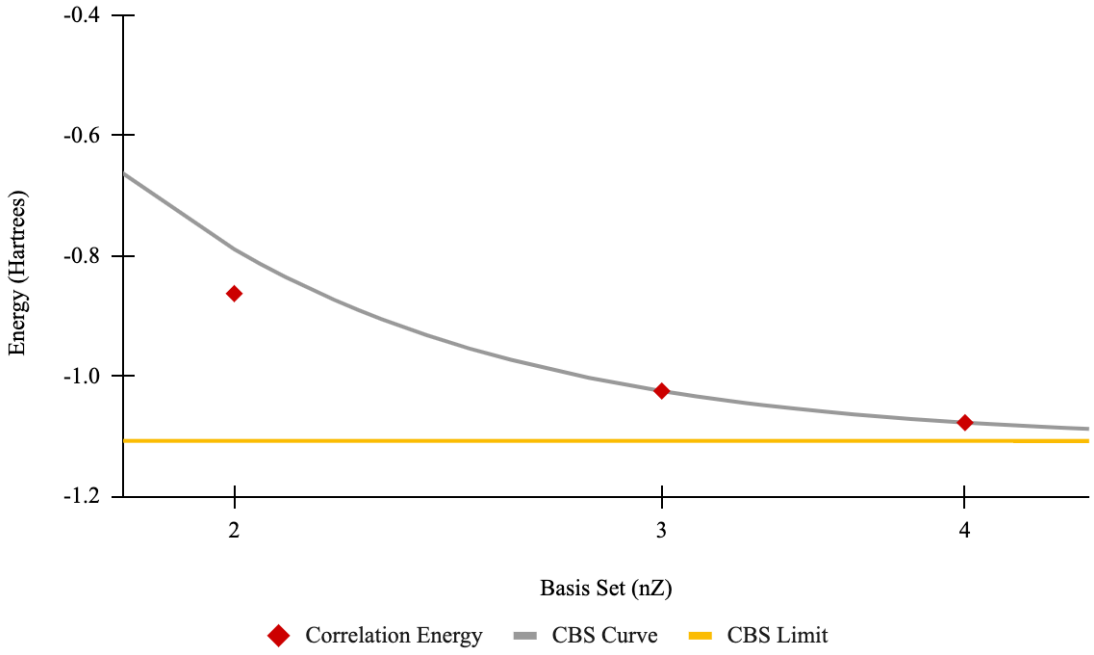


**Figure 2.2 – Systematic Convergence to the CBS Limit for the Correlation Energy of $UO_2$**

$\Delta E_{SO}$ is associated with "spin-same-orbit" SO coupling. This is calculated by taking the difference between a 4-component calculation with the Dirac-Coulomb Hamiltonian[70] and an analogous calculation using the Dyall spin-free Hamiltonian[70] with uncontracted cc-pVDZ-X2C or cc-pVTZ-X2C basis sets. If the system is dominated by the HF determinant with few unpaired electrons, this can be carried out at the CCSD(T) level of theory. However, when the

wavefunction is strongly multi-determinantal, multireference configuration interactions, KRCI/MRCI, will be used instead to recover these spin-orbit effects. $\Delta E_{Gaunt}$ is the contribution associated with "spin-other-orbit" SO coupling. This is calculated as the difference between 4-component Dirac-Hartree-Fock (DHF) calculations using the Dirac-Coulomb-Gaunt and Dirac-Coulomb Hamiltonians, respectively, with uncontracted cc-pVDZ-X2C or cc-pVTZ-X2C basis sets. These calculations are carried out using the DIRAC program.[71]

$\Delta E_{QED}$ is the contribution associated with the leading term of quantum electrodynamics, the Lamb shift, which includes vacuum polarization and self-energy contributions. This is calculated as the difference between a FC-CCSD(T) calculation with cc-pwCVTZ-X2C basis sets with and without the Lamb shift operator applied using a model potential approach first proposed by Zhao and Pyykkö.[27,72] Finally, $E_{ZPE}$ is the contribution associated with zero-point vibrational energy. For diatomics, this can easily be calculated from the CBS limit harmonic frequencies and anharmonicity constants (Equation 2.4). For larger molecules, the ZPE is calculated at the harmonic level with cc-pVTZ-X2C basis sets at the HF/CCSD(T) level of theory. Both of these final contributions are calculated in MOLPRO.[65–67]

$$\mathrm{ZPE} = \frac{1}{2}\omega_e - \frac{1}{4}\omega_e x_e \tag{2.4}$$

When computationally feasible, correlation methods beyond CCSD(T) have been used, i.e., full iterative triples (CCSDT) and CCSDT(Q). Since these scale with the system size M as roughly $M^8$ and $M^{10}$, respectively, these have been used for only the smallest molecules of this work and generally with cc-pVTZ-X2C and cc-pVDZ-X2C basis sets, respectively. These calculations are carried out using the MRCC program[73,74] as interfaced to MOLPRO.

**Relativistic Effects**

As atoms become heavier, relativistic effects must be considered. This is due to a 1s electron of a high Z atom having a larger relativistic mass than a light Z atom due to its velocity approaching the speed of light. With $m_e \propto a_0^{-1}$, the increase in $m_e$ results in s-type orbital contractions across all principal quantum numbers due to orthogonality constraints. Maintaining orthogonality also results in a slight contraction of p-type orbitals and expansion of d- and f-type orbitals. The Dirac Equation contains these effects (Equation 2.5).

$$[\beta' mc^2 + c(\boldsymbol{\alpha} \cdot \boldsymbol{p}) + V]\Psi = \mathrm{E}\Psi \tag{2.5}$$

By solving for the total solution of this 4-component equation, it is found the electron solution is typically larger than the positron solution, leading to large component ($\Psi_L$) and small component ($\Psi_S$) terminology for the electron and positron solutions, respectively. When solving, generally $\Psi_S \sim \frac{Z}{2mc}\Psi_L$ for 1s electrons. For light atoms, this[1] is insignificant. For heavier atoms, such as U (Z=92), $\Psi_S$ is roughly a third of the size of $\Psi_L$, so it must be considered in thermochemical calculations.[6] By rewriting the Dirac Equation while explicitly including the potential energy of the nuclei V, and $E\text{-}V << 2mc^2$, $\Psi_L$ is renormalized and includes relativistic effects (Equation 2.6). If the spin-orbit term is ignored, the equation collapses to a 1-component equation with scalar effects, i.e., the mass-velocity correction $\left(-\frac{p^4}{8m^3c^2}\right)$ and the Darwin correction $\left(\frac{Z\pi\delta(r)}{2m^2c^2}\right)$. $\Psi_L$ can be decoupled from $\Psi_S$ using a unitary transformation so that they are related by an energy-independent matrix "X" constructed from a finite basis set: $\Psi_S = X\Psi_L$.[6] This produces an eXact-2-Component (X2C) transformed Hamiltonian,[75] which is included in the basis sets used. This requires solving the 1-electron Dirac Equation for heavy atoms, but this

is less computationally expensive than 2-electron integral calculations found in non-relativistic Hartree-Fock calculations.

$$\left[\frac{p^2}{2m} + V - \frac{p^4}{8m^3c^2} + \frac{Z\, s\cdot\ell}{2m^2c^2r^3} + \frac{Z\pi\delta(r)}{2m^2c^2}\right]\Psi_L = E\Psi_L \tag{2.6}$$

Another way the small and large components can be decoupled is by performing a sequence of unitary transformations: $U = U_n \ldots U_2U_1U_0$.[6] This eliminates the off-diagonal $\Psi_L{\cdot}\Psi_S$ coupled terms. Often only 3 $U_i$ are used to transform the Hamiltonian, which is then known as a Douglas Kroll 3 (DK3) transformed Hamiltonian.[76–79]

Spin-orbit calculations can be broken down into two categories: SSO coupling and SOO coupling. SSO coupling is calculated, as stated above, with the Dirac-Coulomb Hamiltonian (Equation 2.7).[70] The Coulomb two-electron operator allows the calculation to occur in an electronic field such that the SSO coupling is defined as the electron spin and the magnetic field of a different charged particle from a static frame of reference.[80]

$$\widehat{H} = \beta' mc^2 + c(\boldsymbol{\alpha}\cdot\mathbf{p}) + V + \frac{e^2}{r_{12}};\ \beta' = \beta - \mathbf{I_4} \tag{2.7}$$

SOO interactions need the vector, not scalar, potential of the second electron. The first-order relativistic correction to the two-electron interaction gives the Coulomb term and the vector potential. This is calculated with the Breit term of the Hamiltonian (Equation 2.8). The Breit contribution can be further broken down into the Gaunt and Gauge terms. The Gaunt term is the larger portion and primarily represents the SOO. It has been noted "for accurate studies of molecular spectra including fine structure it is recommended to include spin-other orbit interaction through the Gaunt"[80] term.

$$g^{B}(1,2) = g^{G}(1,2) + g^{gauge}(1,2) = -\frac{ec\boldsymbol{\alpha}_1 \cdot ec\boldsymbol{\alpha}_2}{c^2 r_{12}} - \frac{(ec\boldsymbol{\alpha}_1 \cdot \nabla_1)(ec\boldsymbol{\alpha}_2 \cdot \nabla_2) r_{12}}{2c^2} \quad (2.8)$$

**Correlation Methods**

The main theory of choice in these calculations, CCSD(T), is based on the Hartree-Fock (HF) method, which is a mean-field approximation that approximates the wavefunction as a single Slater determinant. This method is advantageous, as it calculates individual orbital energies, is computationally inexpensive ($\mathcal{O}(m^4)$ from calculating 2-electron integrals) and can recover about 99% of the total energy.[6,81] Variationally, it is the best single determinant wavefunction.

The difference between the exact and HF energy is known as the correlation energy, and it has been found to be critical in describing accurate thermochemical and spectroscopic values.[68] To recover most of the correlation energy, this work utilizes coupled cluster theory with singles, doubles, and perturbative triples (CCSD(T)). CC theory includes excited Slater determinants via a cluster operator, which produces determinants that are singly, doubly, triply, etc. excited up to N-excited, where N is the total number of electrons in the system.[82,83] This operator is applied to the ground state HF wavefunction. When only single and double excitations are incorporated to all orders, this produces what is known as the CCSD level of theory. Thus, $E_{CC}$ is the sum of the HF energy and the correlation energy obtained from the CC calculation. While including higher-electron excitations would give a more accurate and complete picture, this can be very computationally expensive. CCSDT, which is CCSD with full triples, has an iterative computational cost of $\mathcal{O}(\mathrm{m}^8)$ where m represents the system size.[6,83] If the triples are added perturbatively, as in CCSD(T), the iterative cost reduces to $\mathcal{O}(m^6)$ with an ($\mathcal{O}(m^7)$ non-iterative step. [6,83]

However, because CC theory is based on a single determinant, it is not appropriate for systems exhibiting multi-reference behavior. Multireference character is typically larger when spin-orbit coupling is included in the Hamiltonian. If CCSD(T) cannot be used for calculating the correlation energy, a good alternative is to use multireference configuration interaction (MRCI)[84] for the spin-free case (spin-orbit not included) and Kramer's restricted configuration interaction (KRCI) when SO is included.[85] These methods utilize a generalized active space (GAS),[85] which is partitioned by symmetry and number of orbitals with restricted excitation levels. In order to obtain a valuable SO contribution, the GAS must be constructed in a consistent manner between MRCI and KRCI.

**NBO**

An NBO analysis[27,86,87] can help determine bonding patterns in the molecule. An NBO is a set of orthonormal localized orbitals that span the entire basis of natural orbitals. These Natural Atomic Orbitals (NAOs) are similar in practice but distinct from MOs. The former are constructed by diagonalizing one-center blocks of the density matrix and eliminating interatomic overlap. The interatomic overlap is eliminated by a weighted scheme to preserve "occupancy-weighted symmetric orthogonalization."[87]

Once the NAO set is created, it is converted via a transformation sequence to one-center and two-center electron pictures (lone pairs and bonds, respectively) most commonly seen in Lewis structures.[88] The NBO bond is defined as a normalized combination of orthogonal NAOs (Equation 2.9).[27] Any non-Lewis like orbitals generally reflect filled antibonding orbitals. The greater the electronic density found in the Lewis-like atomic orbitals, the better the system is described by a Lewis structure. Since core electrons are not correlated, these orbitals should be

filled. NBO actinide calculations need to have the actinide core manually set to 39 orbitals, so that the 6s and 6p orbitals will appear in the lone pair (LP) group of the calculation.[27]

$$\mathrm{Bond}_{AB} = c_A h_A + c_B h_B \tag{2.9}$$

**Basis Sets**

A basis set is a collection of one-electron functions that are used to analytically represent atomic and molecular orbitals.[6,72,82] The one-electron functions generally follow the functional form $Y(\theta,\phi)\,R(r)$, where $R(r)$ is generally a Gaussian function (Equation 2.10) while $Y(\theta,\phi)$ are the spherical harmonics.[6]

$$R(r) = r^{2n-2-l}e^{-\zeta r^2} \tag{2.10}$$

While Gaussian functions do not have the correct asymptotic dependence for atomic and molecular wavefunctions, e.g., no electron-nuclear cusp, linear combinations of Gaussians can closely over this deficiency. Generally, these linear combinations, or contractions, use fixed contraction coefficients based on atomic calculations.

Ideally, an infinite or complete basis set (CBS) should be used to describe the wavefunction and this would lead to an exact solution for the chosen method, e.g., HF or CCSD(T).[6] However, this is not computationally feasible. Therefore, a finite basis set must be used, which introduce 1-particle errors into the calculation.

To eliminate this basis set incompleteness error (BSIE), a series of basis sets can be used that are extrapolated to the CBS limit. Correlation consistent (cc) basis sets[27,68,69,89–92] are the most common choice of basis sets that can be accurately extrapolated to the CBS limit. These sets are designed to systematically converge both the HF and correlation energies in atomic and molecular calculations. Correlation consistent basis sets, e.g., cc-pV*n*Z, converge to the CBS

limit as the cardinal number *n* of the set increases. At each increase in n, e.g., *n=2* for double-zeta (DZ) and *n=3* for triple-zeta (TZ), a larger set of Gaussians describing the occupied orbitals are used, which works to converge the HF part of the wavefunction, and additional functions for electron correlation are added. The latter, which involve both the same angular momenta as the occupied orbitals but also higher angular momenta to provide both radial and angular correlation, are done systematically such as each new function contributes similar amounts of correlation energy. These "correlation consistent groupings" lead to near exponential convergence of the correlation energy towards the CBS limit as *n* is increased.

Augmentations of these basis sets can allow for more accurate calculations, depending on the thermochemical properties at hand. Augmented basis sets, e.g., aug-cc-pVnZ-X2C, contain diffuse functions, which are basis functions with small exponents (<1).[89] These functions are essential for describing systems with anionic character, such as calculating electron affinities. To recover the electron correlation in core correlated calculations, the chosen basis sets must accurately describe the wave function in the core orbital region. These basis sets contain additional functions with large exponents, known as tight functions, which make these calculations possible.[6] The present work used the so-called weighted core-valence basis sets[93] to determine $\Delta E_{CV}$. In these sets the additional tight functions were optimized with a bias towards recovering core-valence correlation at the expense of core-core, which improves convergence to the CBS limit of the CV contributions to thermochemical properties.

# CHAPTER THREE: THORIUM OXIDE, THORIUM PLATINUM, AND ISOLOBALITY

## Introduction

Actinide chemistry has been of interest in the scientific community for quite some time. Thorium has been given more attention due to its possible associations with developing nuclear energy with it rather than uranium or plutonium.[94–97] Even though no f-orbitals are occupied in its ground state configuration, thorium still has enough complexity with its relativistic effects and large electron count that experiment and computation must work together to get the complete picture of a thorium system.

While most attention is given to its use with oxides in nuclear fuel development, there has been excitement stirring involving metalloactinyls, where their actinide-transition metal bonds remain mostly unexplored. Hoffman's isolobal principle, which states fragments are isolobal "if the number, symmetry properties, approximate energy and shape of the frontier orbitals and the number of electrons in them are similar,"[48] gives a starting point for looking at metalloactinyl molecules, such as comparing Au with F.[97] Work has begun with these metalloactinyls, where triatomic structures with a thorium or uranium center with either F substituted by Au or O replaced by Pt were analyzed.[27,97] However, less work has been carried out on the diatomic metalloactinyls, with previous work only carried out with DFT or CASPT2.[98–100] Thus, the purpose of this work is to see if isolobality still applies for diatomic metalloactinyls; if high accuracy computational methods can describe the systems well; and provide a basis for the benefits of the FPD procedure on actinide electron affinities, which have not been widely analyzed for small molecules.[21,22,24,25,47]

Calculation of the ThO and ThPt electron affinities was undertaken in this work, building off the previous work of Li et. al.,[17] where the vertical electron affinity (VEA) of ThO was measured via photoelectron imaging spectroscopy[17,101] with supporting ab initio calculations. The FPD procedure has characterized other thermochemical properties of ThO[39], such as its IP and BDE, but not its electron affinity. Using the well-characterized ThO/$ThO^-$ system as a benchmark, the FPD procedure will be used to predict the electron affinity of ThPt and analyze its similarities to ThO.

**Computational Details**

The Feller-Peterson-Dixon (FPD) method has been implemented in the following manner (Equation 3.1) to best describe the system at 0 K. Most of these calculations were performed at the CCSD(T) level of theory with the DK3 Hamiltonian and aug-cc-pVXZ-DK basis sets for O and cc-pVXZ-DK3 for Th and Pt,[27,69] with diffuse functions added by including even tempered functions for Th and Pt. These combinations of basis set will be denoted as cc-pVxZ-DK3+ below. Core-valence calculations incorporated weighted CV basis sets (e.g., cc-pwCVXZ-DK3) with otherwise the same schema. Geometries were optimized at the CCSD(T)/CBS(wCV) level of theory. This geometry was used to calculate the other contributions. All but the spin-orbit-related calculations were performed with the MOLPRO quantum chemistry package,[65–67] and the spin-orbit-related calculations were performed with DIRAC.[71]

$$E_{FPD} = E_{VQZ} + \Delta E_{CBS} + \Delta E_{CV} + \Delta E_{SO} + \Delta E_{Gaunt} + \Delta E_{QED} + \Delta E_{T,Q} + \Delta E_{VEA} + E_{ZPE} \quad (3.1)$$

$E_{VQZ}$ is the base energy calculation at the frozen-core FC-CCSD(T)/cc-pVQZ-DK3+ level. $\Delta E_{CBS}$ was calculated using cc-pVTZ-DK3+ and cc-pVQZ-DK3+ using the CBS extrapolation formulas described in Chapter 2. $\Delta E_{CV}$ was obtained by extrapolating to the CBS

limit using cc-pwCVTZ-DK3+ and cc-pwCVQZ-DK3+ basis sets. The outer-core was defined as the 1s orbital for O; 5s, 5p, and 5d orbitals for Th; and 5s and 5p orbitals for Pt. $\Delta E_{QED}$ was calculated with cc-pwCVTZ-DK3+ basis sets (c.f., Ch.2), and $E_{ZPE}$ was calculated using the FC CBS limit's harmonic frequencies and anharmonicity constants. The latter were obtained via 2$^{nd}$-order vibrational perturbation theory using force constants obtained from polynomial fits to 7 unequally distributed points around the equilibrium bond lengths on each potential energy function.

$\Delta E_{SO}$ was calculated at the optimized CCSD(T)/CBS(wCV) geometry. Uncontracted cc-pVTZ-DK3+ basis sets were used. For the open-shell atoms and molecules, the average-of-configuration Dirac Hartree-Fock (AoC-DHF) consisted of 2 electrons in 10 6d spinors for Th; 10 electrons in 2 6s and 10 5d spinors for Pt; and 1 electron in 2 6d spinors for Th in $ThO^-$ and $ThPt^-$. The resulting CCSD(T) calculations, spin-free and with spin-orbit, were carried out on the ground electronic state while correlating the outer-core with a virtual cut-off of 12.0 a.u. The $\Delta E_{SO}$ associated with the fine-structure splitting of oxygen atom was not calculated in this manner but was determined from the J-average of its experimental splitting. $\Delta E_{Gaunt}$ was calculated with the same AoC-DHF parameters and with the Hamiltonians described in Chapter 2. These were only performed at the AoC-DHF level of theory with cc-pVTZ-DK3+ basis sets.

Due to the relatively small size of these diatomics, it was feasible to perform calculations that used a higher level of coupled cluster theory. Two sets of calculations determined the difference of CCSDT and CCSD(T) with cc-pVTZ-DK3+ basis sets and the difference of CCSDT(Q) and CCSDT with cc-pVDZ-DK3+ sets. These two differences, $\Delta E_T$ and $\Delta E_Q$,

respectively, were combined into one contribution, $\Delta E_{T,Q}$, for determining the final FPD electron affinities and bond dissociation energies.

Since the experimental results of the electron affinity of ThO is really a vertical electron affinity (VEA), and the above contributions were calculated for the adiabatic EA, a contribution $\Delta E_{VEA}$ was included to approximately correct the total adiabatic EA to a VEA. This involved calculating the neutral molecule at the anion's optimized geometry at the CCSD(T)/cc-pwCVTZ-DK3+ level of theory, determining the difference between these calculations and the equilibrium calculations at the same level of theory. It should be noted that the VEA neglects any ZPE contributions.

**Results and Discussion**

The optimized bond lengths for each molecule are shown in Table 3.1. As predicted, ThO and ThPt, as well as $ThO^-$ and $ThPt^-$ were found to have the same electronic ground states, with the extra electron of the anion found in a Th 6d orbital. Thus, isolobality seems to qualitatively apply to O and Pt when bonded to Th. The bond lengths of ThO can be compared to previous findings,[17] which at the CCSD(T) level were calculated to be 1.845 Å and 1.890 Å, which agree with the current CCSD(T) calculated bond lengths shown in Table 3.1.

**Table 3.1 – Electronic and Geometric Structures**

| Molecule | Electronic State | r, Th-O/Pt (Å) |
|---|---|---|
| **ThO** | $^1\Sigma^+$ | 1.8400 |
| **$ThO^-$** | $^2\Delta$ | 1.8835 |
| **ThPt** | $^1\Sigma^+$ | 2.3630 |
| **$ThPt^-$** | $^2\Delta$ | 2.4243 |

The final FPD adiabatic and vertical electron affinities, along with the individual FPD contributions, are shown in Tables 3.2 (ThO) and 3.3 (ThPt). For ThO, the calculated adiabatic and vertical electron affinities were found to be 0.69 eV (15.95 kcal/mol) and 0.71 eV (16.39 kcal/mol), respectively, which are in excellent agreement with the experimental VEA of 0.707 eV ± 0.020. The ThPt adiabatic and vertical electron affinities were calculated to be 1.14 eV (26.14 kcal/mol) and 1.17 eV (26.75 kcal/mol), respectively. Based on the current FPD results for ThO, the uncertainty in the predicted EA of ThPt is estimated to be 0.02 eV.

**Table 3.2 – Electron Affinities, Adiabatic and Vertical, in eV (kcal/mol) for ThO**

| EA | $E_{VQZ}$ | $\Delta E_{CBS}$ | $\Delta E_{CV}$ | $\Delta E_{SO}$ | $\Delta E_{Gaunt}$ | $\Delta E_{QED}$ | $\Delta E_{T,Q}$ | $E_{ZPE}$ | $\Delta E_{VEA}$ | FPD | Exp. |
|---|---|---|---|---|---|---|---|---|---|---|---|
| **Adia.** | 0.58 (13.27) | 0.00 (0.10) | -0.07 (-1.50) | 0.13 (3.02) | 0.00 (0.09) | 0.01 (0.29) | 0.03 (0.56) | 0.01 (0.12) | - | 0.69 (15.95) | 0.707 ± 0.020 (16.30 ± 0.46) |
| **Vert.** | 0.58 (13.27) | 0.00 (0.10) | -0.07 (-1.50) | 0.13 (3.02) | 0.00 (0.09) | 0.01 (0.29) | 0.03 (0.56) | - | 0.02 (0.56) | 0.71 (16.39) | |

For both ThO and ThPt, $\Delta E_{CBS}$ is very small at 0.10-0.16 kcal/mol. This indicates the VQZ+ calculation is close to the CBS limit. Correlating the outer core was very important for both systems, as it lowered the overall EAs by over 1 kcal/mol. $\Delta E_{SO}$ was the largest contribution by far at 3.02 kcal/mol and 4.20 kcal/mol for ThO and ThPt, respectively. This makes sense, as the system in both instances are adding a d electron, which will have significant SO coupling compared to the closed-shell neutral molecules. $\Delta E_{Gaunt}$ is relatively small, but it is twice as large for the EA of ThPt than for ThO. The heavier nature of platinum may be playing into this. $\Delta E_{QED}$ has roughly the same value for both instances and is relatively small. The higher orders of coupled cluster theory (CCSDT(Q) and CCSDT) found in $\Delta E_{T,Q}$ were essential in providing an accurate electron affinity, increasing the FPD total by over 0.5 kcal/mol in both cases, which is

comparable to the stated experimental uncertainty of 0.46 kcal/mol for the EA of ThO. This shows how important, when feasible, it is to include these terms in composite accurate calculations.

**Table 3.3 – Electron Affinities, Adiabatic and Vertical, in eV (kcal/mol) for ThPt**

| EA | $E_{VQZ}$ | $\Delta E_{CBS}$ | $\Delta E_{CV}$ | $\Delta E_{SO}$ | $\Delta E_{Gaunt}$ | $\Delta E_{QED}$ | $\Delta E_{T,Q}$ | $E_{ZPE}$ | $\Delta E_{VEA}$ | FPD |
|---|---|---|---|---|---|---|---|---|---|---|
| **Adia.** | 0.97 (22.27) | 0.01 (0.16) | -0.05 (-1.24) | 0.18 (4.20) | 0.01 (0.16) | 0.01 (0.32) | 0.01 (0.23) | 0.00 (0.04) | - | 1.14 (26.14) |
| **Vert.** | 0.97 (22.27) | 0.01 (0.16) | -0.05 (-1.24) | 0.18 (4.20) | 0.01 (0.16) | 0.01 (0.32) | 0.01 (0.23) | - | 0.03 (0.65) | 1.17 (26.75) |

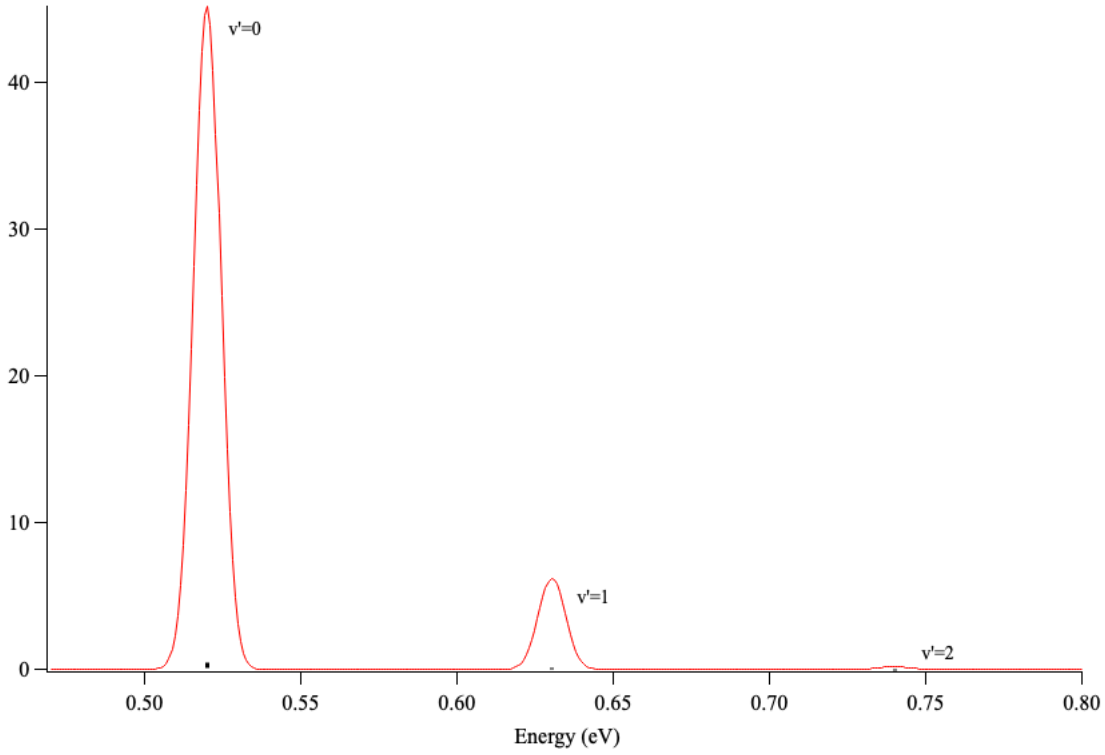


**Figure 3.1 – Franck-Condon Factors for ThO at CCSD(T)/wCV(CBS) Level of Theory**

A few distinct Franck-Condon factors were located for ThO at the CV/CCSD(T) CBS(wCV) level of theory (Figure 3.1). This was performed with the Level[102] program. Three vibrational peaks were distinct enough to notice, all from the vibrational ground state of $ThO^-$:

v'=0, at 0.52 eV; v'=1 at 0.63 eV; and v'=2 at 0.74 eV Including the various FPD contributions would shift these peaks to EA values larger by 0.19 eV. These agree well with the FC simulation done by Li et al.,[17] which was performed at 1064 nm and 532 nm via the PESCAL program.[103]

The 0 K bond dissociation energies BDEs were also calculated for ThO and ThPt (Table 3.4) using FPD and found to be 9.02 eV (207.95 kcal/mol) and 5.91 eV (136.37 kcal/mol), respectively. There are no experimental values for ThPt, but there is for ThO (207.6 ± 1.2 kcal/mol)[23] and previous theoretical work[19,39] on the BDE of ThO has been done. The ThO BDE calculated in this thesis is essentially identical to the results of the FPD calculations of Ref.[39] and the experimental measurement. The BDE of ThPt is roughly 33% smaller than the BDE of ThO.

**Table 3.4 – Bond Dissociation Energies in eV (kcal/mol) for ThO and ThPt**

| BDE | $E_{VQZ}$ | $\Delta E_{CBS}$ | $\Delta E_{CV}$ | $\Delta E_{SO}$ | $\Delta E_{Gaunt}$ | $\Delta E_{QED}$ | $\Delta E_{T,Q}$ | $E_{ZPE}$ | FPD |
|---|---|---|---|---|---|---|---|---|---|
| **Th-O** | 9.27 (213.71) | 0.09 (2.15) | 0.13 (3.02) | -0.39 (-9.05) | 0.02 (0.37) | 0.00 (0.03) | -0.04 (-1.01) | -0.06 (-1.27) | 9.02 (207.95) |
| **Th-Pt** | 6.47 (149.23) | 0.06 (1.46) | 0.18 (4.13) | -0.74 (-16.98) | -0.02 (-0.48) | -0.03 (-0.63) | -0.11 (-2.49) | -0.02 (-0.35) | 5.91 (136.37) |

Here $\Delta E_{CBS}$ is quite large, being over 1 kcal/mol for both ThO and ThPt. While the CBS limit was not mission critical for determining electron affinities that were only one electron apart, dissociating a bond appears to necessitate going to the CBS limit to remove the 1-electron error associated with finite basis sets. $\Delta E_{CV}$ is very large, at 3-4 kcal/mol. For EAs and for BDEs, this contribution has more influence on the overall calculation than the CBS limit, though both are clearly important. $\Delta E_{SO}$ is at least three times larger in magnitude than any other contribution. It is also negative for both molecules, as they are breaking into their atomic forms, which are much higher in spin. The ThPt $\Delta E_{SO}$ is much larger in magnitude than ThO $\Delta E_{SO}$, which is due to

the higher SO coupling occurring in atomic Pt over atomic O. $\Delta E_{Gaunt}$ has similar magnitudes, but opposite signs. $\Delta E_{QED}$ is almost negligible for ThO, but decreases ThPt by 0.63 kcal/mol. This implies the s electron population decreases (the scalar relativistic effects decrease) when dissociating Th and Pt. $\Delta E_{T,Q}$ is even larger here than for the electron affinities, as it lowers the ThO BDE by over 1 kcal/mol and 2.49 kcal/mol for ThPt. This again emphasizes the importance of including higher order theory contributions when applicable. Without these, the BDEs would be much too large. Finally, $E_{ZPE}$ decreases each BDE, as expected, by -1.27 kcal/mol for ThO and -0.35 kcal/mol for ThPt.

*Natural Bond Order Analysis*

**Table 3.5 – NBOs of the Lewis Structures of ThO and $ThO^-$**

| | | | | | | Hybrid Character | | | |
|---|---|---|---|---|---|---|---|---|---|
| **Mol.** | **q(Th/O)** | **Type** | **Occupancy** | **% Ion** | **Center** | **%s** | **%p** | **%d** | **%f** |
| **ThO** | 1.36 | $n_{Th}$ | 1.929 | | Th | 95 | 1 | 3 | 0 |
| | /-1.36 | $n_O$ | 1.994 | | O | 79 | 21 | 0 | 0 |
| | | $\sigma_{ThO}$ | 2.000 | 67.9 | Th | 3 | 4 | 62 | 31 |
| | | | | | O | 21 | 78 | 0 | 0 |
| | | $\pi_{ThO}$ | 2.000 | 80.5 | Th | 0 | 0 | 71 | 28 |
| | | | | | O | 0 | 100 | 0 | 0 |
| **$ThO^-$** | 0.41 | $n_{Th}$ | 1.000 | | Th | 0 | 0 | 99 | 1 |
| | /-1.41 | $n_{Th}$ | 1.992 | | Th | 94 | 4 | 1 | 0 |
| | | $n_O$ | 1.992 | | O | 77 | 23 | 0 | 0 |
| | | $\sigma_{ThO}$ | 2.000 | 70.0 | Th | 2 | 4 | 67 | 27 |
| | | | | | O | 24 | 75 | 0 | 0 |
| | | $\pi_{ThO}$ | 2.000 | 81.7 | Th | 0 | 0 | 76 | 23 |
| | | | | | O | 0 | 100 | 0 | 0 |

A molecular orbital and bond analysis has been performed previously by Li et al. on ThO and $ThO^-$,[17] where it was determined that O 2p, Th 7s, and Th 6d combine to form σ and π bonds. In $ThO^-$, the singly occupied orbital was determined to correspond to a Th 6d orbital, as

the current calculations have also shown. An NBO analysis, as described in Chapter 2, was performed on these molecules (Table 3.5). Besides the aforementioned four Th orbitals (6s and 3 6p orbitals), ThO was found to have 2 remaining lone pairs, one on Th and one on O. The Th lone pair is a predominantly Th 7s orbital, while the lone pair on O is a 2s2p hybrid (79% s, 21% p). The molecule contains one σ bond and one π bond, where the bonds are ionized towards oxygen. For the σ bond, the Th orbitals are predominantly a df hybrid (3% s, 4% p, 62% d, 31% f), while the O orbitals are a sp hybrid (21% s, 78% p). The π bond is between a Th df hybrid (71% d, 28% f) and an exclusively O 2p orbital. $ThO^-$ has similar bonding to ThO. The anion electron is found in a predominantly Th 6d orbital. The Th 7s orbital and O 2s2p orbital are also fully filled, as well as the Th 6s and 3 6p orbitals. The σ bond and π bonds are slightly more ionized towards oxygen than in the neutral, with similar orbital mixes participating in bonding.

An NBO analysis, as described in Chapter 2, was also performed for ThPt and $ThPt^-$ (Table 3.6). Besides the aforementioned four Th orbitals (6s and 3 6p orbitals), 1 lone pair on Th and 3 lone pairs on Pt were identified for ThPt: Th 7s, two Pt 5d, and one Pt 6s5d hybrid (36% s, 63% d). There is one σ bond and one π bond in ThPt, where the bonds are both ionized towards Pt. For the σ bond, the Th orbitals have majority d character (more than on its oxygen counterpart), while the Pt are a sd hybrid (63% s, 36% d). For the π bond, this is between a Th df hybrid (75% d, 24% f) and an exclusively Pt 5d orbital. $ThPt^-$ has a similar NBO analysis to ThPt. Here, as predicted, the anion electron is found in a Th 6d orbital. The Th 7s orbital is filled, and there are three lone pairs on Pt: two in 5d orbitals and one in a sd hybrid (55% s, 45% d). A σ bond and π bond are also found in this molecule, though they are more polarized towards Pt than the neutral. Here the σ bond is a combination of a predominantly Th 6d orbital and a Pt sd

hybrid (45% s, 55% d), while the π bond is a combination of a Th df hybrid (77% d, 22% f), and an exclusively Pt 5d orbital. This makes sense given the isolobality shown between Pt and O.

**Table 3.6 – NBOs of the Lewis Structures of ThPt and $ThPt^-$**

| | | | | | | Hybrid Character | | | |
|---|---|---|---|---|---|---|---|---|---|
| **Mol.** | **q(Th/Pt)** | **Type** | **Occupancy** | **% Ion** | **Center** | **%s** | **%p** | **%d** | **%f** |
| **ThPt** | 1.03 | $n_{Th}$ | 1.981 | | Th | 92 | 3 | 5 | 1 |
| | /-1.03 | $n_{Pt}$ | 1.980 | | Pt | 0 | 0 | 100 | 0 |
| | | $n_{Pt}$ | 1.980 | | Pt | 0 | 0 | 100 | 0 |
| | | $n_{Pt}$ | 1.955 | | Pt | 36 | 0 | 63 | 0 |
| | | $\sigma_{ThPt}$ | 2.000 | 54.5 | Th | 4 | 3 | 88 | 4 |
| | | | | | Pt | 63 | 0 | 36 | 0 |
| | | $\pi_{ThPt}$ | 2.000 | 77.4 | Th | 0 | 1 | 75 | 24 |
| | | | | | Pt | 0 | 0 | 100 | 0 |
| **$ThPt^-$** | 0.29 | $n_{Th}$ | 1.013 | | Th | 0 | 0 | 99 | 1 |
| | /-1.29 | $n_{Th}$ | 1.956 | | Th | 96 | 3 | 0 | 0 |
| | | $n_{Pt}$ | 1.987 | | Pt | 0 | 0 | 100 | 0 |
| | | $n_{Pt}$ | 1.987 | | Pt | 0 | 0 | 100 | 0 |
| | | $n_{Pt}$ | 1.961 | | Pt | 55 | 0 | 45 | 0 |
| | | $\sigma_{ThPt}$ | 2.000 | 69.4 | Th | 2 | 4 | 85 | 9 |
| | | | | | Pt | 45 | 0 | 55 | 0 |
| | | $\pi_{ThPt}$ | 2.000 | 80.9 | Th | 0 | 1 | 77 | 22 |
| | | | | | Pt | 0 | 0 | 100 | 0 |

## Conclusions

In this chapter, the electron affinities of ThO and ThPt, as well as their corresponding bond dissociation energies, have been studied using the FPD procedure. The calculated vertical electron affinity of ThO (0.71 eV) is in excellent agreement with the previous experimental result by Li et al (0.707 ± 0.020 eV).[17] The isolobality of O and Pt is present when bonding to the heavy element thorium, as the electronic structures of ThO and ThPt, and $ThO^-$ and $ThPt^-$, are essentially identical. The electron affinity of ThPt is significantly higher than the electron

affinity of ThO, while its BDE is roughly two-thirds the size of the BDE of ThO. The NBO analyses performed on all four molecules show the bonding is similar between Th and O and Th and Pt, with more ionicity and 5f orbital bonding participation occurring in ThO/$ThO^-$ than ThPt/$ThPt^-$.

# CHAPTER FOUR: DETERMINING GEOMETRIC AND ELECTRONIC STRUCTURE FOR METALLOACTINYL SPECIES

## Introduction

Anion photoelectron spectroscopy (APS) involves the excitation of an anion with a fixed frequency photon,[104] which ejects an electron, leaving the neutral molecule in its ground or excited electronic state.[105] The kinetic energy of the ejected electron is measured, and energy conservation yields the electron binding energy, which is directly related to the electron affinity. Bowen at Johns Hopkins University has been utilizing this method to determine electron affinities of various metalloactinyl species,[18,44,97] including ones involving thorium and platinum.

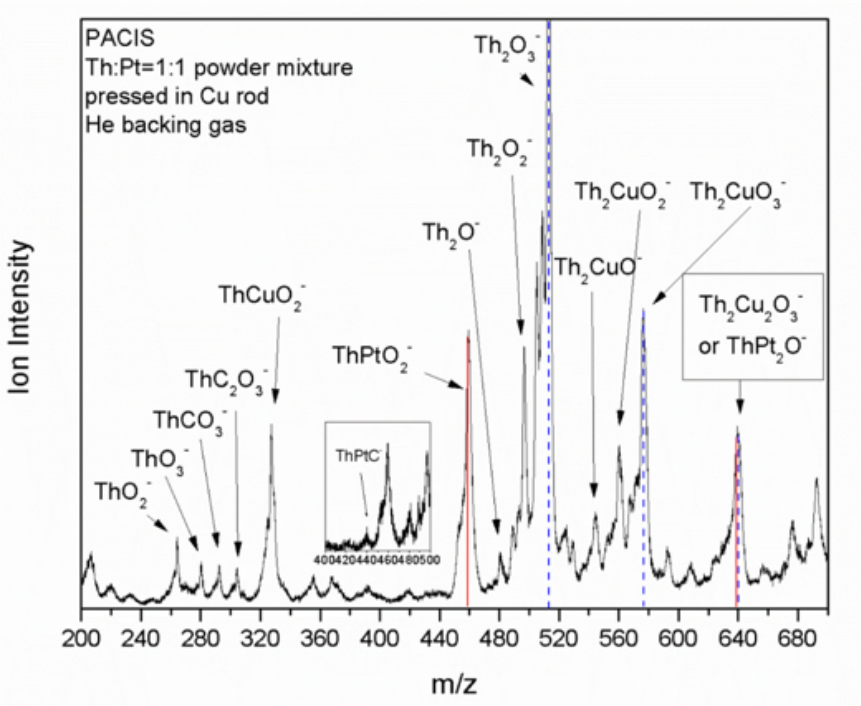


**Figure 4.1 – Mass Spectrometry Results for reaction of Thorium, Platinum, and Copper [106]**

In one experiment, a thorium-platinum powder mixture (in a 1:1 ratio) was pressed onto a copper rod to create Th, Pt, and Cu rich compounds. A PACIS (pulsed arc cluster ion source)

sent the negatively charged ions formed to the TOF mass spectrometer, where selected ions were sent to be analyzed via APS. The mass spectrometer reading (Figure 4.1) and APS spectrum (Figure 4.2) show that a small amount of $ThPtC^-$ was created, with a vertical detachment energy (VDE) of roughly 1.5 eV. This is all the information on the given system. In this chapter, the goal will be to determine the geometric structure of $ThPtC^-$ and ThPtC, as well as accurately calculate the adiabatic electron affinity (AEA), vertical detachment energies, electronic structures, and bonding patterns of these molecules via the relativistic FPD procedure.

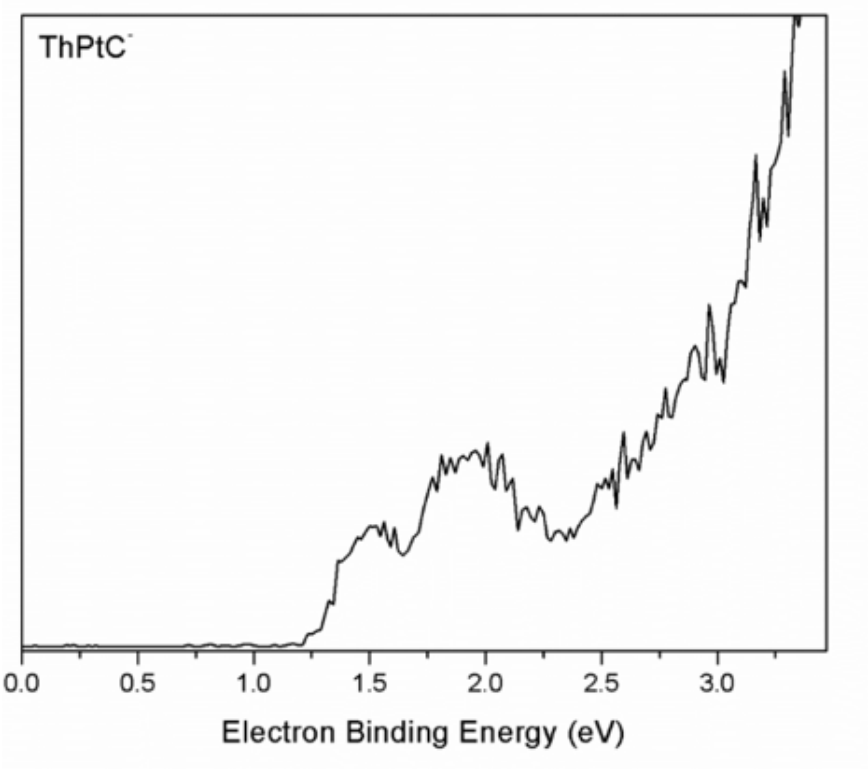


**Figure 4.2 – Anion Photoelectron Spectrum of $ThPtC^-$ [106]**

**Computational Methods**

The Feller-Peterson-Dixon (FPD) method has been implemented as shown in Equation 4.1. Most of these calculations were performed at the CCSD(T) level of theory with the DK3 Hamiltonian and aug-cc-pVXZ-DK basis sets for C and cc-pVXZ-DK3 for Th and Pt (X=D-Q),[27,69] with additional diffuse functions added for Th and Pt. These combinations will be denoted as cc-pVXZ-DK3+ below. Core-valence calculations incorporated weighted CV basis sets (e.g., aug-cc-pVXZ-DK and cc-pwCVXZ-DK3), all with additional diffuse functions. Linear molecules were optimized at the frozen core (FC)-CCSD(T)/cc-pVQZ-DK+ level of theory, while bent molecules were optimized at the FC-CCSD(T)/cc-pVTZ-DK+ level of theory. All contributions of Eq. 4.1 used these geometries. All but the spin-orbit-related calculations were performed with the MOLPRO quantum chemistry package,[65–67] and the spin-related calculations were performed with DIRAC.[71]

$$E_{FPD} = E_{VQZ} + \Delta E_{CBS} + \Delta E_{CV} + \Delta E_{SO} + \Delta E_{Gaunt} + \Delta E_{QED} + E_{ZPE} \quad (4.1)$$

$E_{VQZ}$ is the base energy calculation at the FC-CCSD(T)/cc-pVQZ-DK3 level. $\Delta E_{CBS}$ was calculated by extrapolating the cc-pVTZ-DK3+ and cc-pVQZ-DK3+ energies using the formulas described in Chapter 2. $\Delta E_{CV}$ was obtained as the difference between valence-only (FC) and valence+outer-core correlated CCSD(T) calculations extrapolated to the CBS limit using cc-pwCVTZ-DK3+ and cc-pwCVQZ-DK3+ basis sets. The outer-core was defined as the 1s orbital for C; 5s, 5p, and 5d orbitals for Th; and 5s and 5p orbitals for Pt. $\Delta E_{QED}$ was calculated at the FC-CCSD(T)/ cc-pwCVTZ-DK3+ level as described in Ch. 2. $E_{ZPE}$ was calculated using FC-CCSD(T)/cc-pVTZ-DK3+ harmonic frequencies but is only included when calculating adiabatic electron affinities.

$\Delta E_{SO}$ was calculated as described in Ch. 2 at the optimized geometry specified above. Uncontracted cc-pVDZ-DK3+ basis sets used. The average-of-configuration Dirac Hartree-Fock (AoC-DHF) calculations corresponded to 2 electrons in 4 spinors of C 2p orbitals for CThPt; 3 electrons in 6 spinors of C 2p and Th 7s orbitals of $CThPt^-$; 2 electrons in 4 spinors of Th 6d orbitals for ThCPt; and 3 electrons in 6 spinors of Th 6d orbitals for $ThCPt^-$. The resulting KRCI/MRCI calculations were performed on the ground electronic states while correlating all the valence electrons except the low-lying 6s of Th. A virtual orbital cutoff of 0.5 a.u. was used. $\Delta E_{Gaunt}$ was calculated with the same AoC-DHF parameters as the difference between DHF calculations with the Dirac-Coulomb-Gaunt and Dirac-Coulomb Hamiltonians. These were only performed at the AoC-DHF level of theory with uncontracted cc-pVDZ-DK3+ basis sets.

To calculate the vertical detachment energies, each contribution each contribution (except the ZPE) of Eq. 4.1 was calculated with the neutral fixed to the optimized anion geometry.

**Results & Discussion**

Previous work[16,18,19] indicated thorium, carbon, and oxygen attached as Th-C-O, although the bent CThO isomer was calculated to lie higher in energy by just 4 kcal/mol. Due to the isolobality of O and Pt, this "carbonyl" arrangement (Th-C-Pt) as well as the "insertion" arrangement (C-Th-Pt) were analyzed. Th-Pt-C was not analyzed due to isolobality implying Pt or O must be at the end of bond to be similar. Table 4.1 shows the geometries of the neutral and anion for each arrangement. In the carbonyl arrangement, the structures were linear with open shell electrons found in C 2p orbitals while the anion electron was found in a Th 6d orbital. The insertion arrangement is distinctly bent for neutral and anion optimized ground state geometries, where again the electron states were found to be a triplet and quartet respectively. Both the

carbonyl and insertion arrangements have two electrons in C 2p orbitals, but the third electron on the anion of the insertion arrangement was determined to be in a Th 7s orbital.

**Table 4.1 – Electronic and Geometric Structures**

| Molecule | Electronic State | r, Th-C (Å) | r, Pt-X (X= Th, C) (Å) | Angle |
|---|---|---|---|---|
| **ThCPt** | $^3\Sigma^-$ | 2.1897 | 1.7658 | 180.0º |
| **ThCPt$^-$** | $^4\Delta$ | 2.2515 | 1.7566 | 180.0º |
| **CThPt** | $^3$A’ | 2.1387 | 2.4129 | 116.33º |
| **CThPt$^-$** | $^4$A’ | 2.1787 | 2.4651 | 118.47º |

Adiabatic electron affinities were calculated for both arrangements (Table 4.2). Even though the geometries are very different, the total ADEs are within 2 kcal/mol of each other, with ThCPt$^-$ being 1.43 eV (32.95 kcal/mol) and CThPt$^-$ 1.35 eV (31.24 kcal/mol). The $E_{VQZ}$ values are both around 1.30 eV. $\Delta E_{CBS}$ increases ThCPt$^-$ by about 0.25 kcal/mol, while it is almost negligible for CThPt$^-$. The $\Delta E_{CV}$ values differ from each other by over 1 kcal/mol and have different signs. Correlating the outer core for the linear arrangement decreases the overall EA by a little less than 1 kcal/mol, while it increases the insertion isomer by 0.25 kcal/mol. $\Delta E_{SO}$ increases the EA for the linear arrangement by over 3 kcal/mol, while the insertion arrangement increases by 0.86 kcal/mol. This makes sense, as the anion electron is placed into a Th 6d orbital for the linear arrangement, which will have more SO coupling than the Th 7s orbital occupied in the insertion isomer. $\Delta E_{Gaunt}$ is almost negligible for ThCPt$^-$ (0.00 eV, 0.05 kcal/mol), but decreases the EA of CThPt$^-$ by -0.01 eV (-0.26 kcal/mol). $\Delta E_{QED}$, like $\Delta E_{CV}$, have differing signs for the different arrangements, where it is positive (0.03 eV, 0.64 kcal/mol) for ThCPt$^-$ and

negative (-0.01 eV, -0.26 kcal/mol) for CThPt⁻. Finally, the $E_{ZPE}$ contributions are nearly negligible in this instance (0.00 eV) for both arrangements.

**Table 4.2 – Adiabatic Electron Affinities in eV (kcal/mol) for ThCPt and CThPt**

| Molecule Adia. | $E_{VQZ}$ | $\Delta E_{CBS}$ | $\Delta E_{CV}$ | $\Delta E_{SO}$ | $\Delta E_{Gaunt}$ | $\Delta E_{QED}$ | $E_{ZPE}$ | FPD |
|---|---|---|---|---|---|---|---|---|
| ThCPt⁻ | 1.29 (29.81) | 0.01 (0.23) | -0.04 (-0.97) | 0.14 (3.12) | 0.00 (0.05) | 0.02 (0.55) | 0.00 (0.09) | 1.43 (32.87) |
| CThPt⁻ | 1.32 (30.44) | -0.00 (-0.03) | 0.01 (0.25) | 0.04[a] (0.86) | -0.01 (-0.26) | -0.01 (-0.12) | 0.00 (0.10) | 1.35 (31.24) |

[a]This number is currently being revised

The vertical detachment energies calculated using FPD are shown in Table 4.3. The final VDEs are found to be 1.47 eV (33.93 kcal/mol) for ThCPt⁻ and 1.49 eV (34.43) for CThPt⁻. Both are very close to experimental (1.50 eV, 34.59 kcal/mol) and fall within the FPD targeted accuracy (0.04 eV, or 1 kcal/mol). The ground state structure is the "insertion" isomer, CThPt⁻. When the difference between ThCPt⁻ and CThPt⁻ is calculated fully with FPD, the different shows CThPt⁻ is lower by 0.34 eV (7.84 kcal/mol).

**Table 4.3 – Vertical Detachment Energies in eV (kcal/mol) for ThCPt and CThPt**

| Molecule VDE | $E_{VQZ}$ | $\Delta E_{CBS}$ | $\Delta E_{CV}$ | $\Delta E_{SO}$ | $\Delta E_{Gaunt}$ | $\Delta E_{QED}$ | FPD | Exp. |
|---|---|---|---|---|---|---|---|---|
| ThCPt⁻ | 1.34 (30.88) | 0.00 (0.14) | -0.02 (-0.57) | 0.15 (3.49) | 0.00 (0.08) | -0.00 (-0.08) | 1.47 (33.93) | 1.50 (34.59) |
| CThPt⁻ | 1.37 (31.62) | 0.01 (0.09) | 0.02 (0.48) | 0.11[a] (2.61) | -0.01 (-0.24) | -0.01 (-0.13) | 1.49 (34.43) | 1.50 (34.59) |

[a]This number is currently being revised

The $E_{VQZ}$ values for both VDEs are about a tenth of an eV lower than their final FPD totals (1.34 eV for ThCPt⁻, and 1.37 eV for CThPt⁻). $\Delta E_{CBS}$ is almost negligible for both, with the insertion isomer's contribution being barely a hundredth of an eV. $\Delta E_{CV}$ changes the VDEs of

both isomers by roughly 0.5 kcal/mol, decreasing that of $ThCPt^-$ and increasing the VDE of $CThPt^-$. Both $\Delta E_{SO}$ contributions increase the VDE by 2-3 kcal/mol. The $\Delta E_{SO}$ values for the AEA and VDE of $ThCPt^-$ are similar, while for $CThPt^-$ the $\Delta E_{SO}$ contribution to its VDE is about three times larger than for the AEA. Thus, at the anion geometry, there is more SO coupling for the neutral, perhaps due to the large change in the Th-Pt bond length, c.f., Table 4.1. $\Delta E_{Gaunt}$ is almost negligible for $ThCPt^-$ (0.00 eV, 0.08 kcal/mol) and only slightly decreases the VDE for $CThPt^-$, -0.01 eV (-0.24 kcal/mol). $\Delta E_{QED}$ is also calculated to be very small for both $ThCPt^-$ (-0.00 eV, -0.08 kcal/mol) and $CThPt^-$ (-0.01 eV, -0.13 kcal/mol).

*Natural Bond Order Analysis*

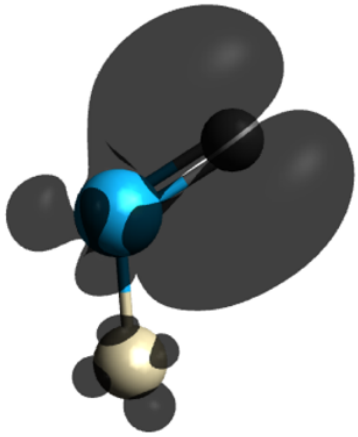

**Figure 4.3 – the SOMO of CThPt and LUMO of $CThPt^-$**

An NBO analysis was performed for the insertion isomers. The neutral LUMO and anion SOMO were almost identical in composition (Figure 4.3). Due to the complicated nature of the open-shell species, the alpha and beta spin portions of the NBO are not combined in the analysis (Table 4.4). However, the energies are similar enough in the spins that it can be concluded that

the two open-shell electrons are in a C s-dominant sp hybrid orbital and a Th-C half bond at -0.4273 au. The MO configuration can be written as seen in Equation 4.2.

$$(n_{Th})^2(n_{Th})^2(n_{Th})^2(n_{Th})^2(n_C)^2(\sigma_{ThC})^2(\pi_{ThPt})^2(\sigma_{ThC})^1(\sigma_{ThPt})^2(n_{Pt})^2(n_{Pt})^2(n_{Pt})^2(n_{Pt})^2(\pi_{ThC})^2 \quad (4.2)$$

**Table 4.4 – NBOs of the Lewis Structure of CThPt**

| | | | | | Th Hybrid (A) | | | | | C/Pt Hybrid (B) | | | |
|---|---|---|---|---|---|---|---|---|---|---|---|---|---|
| **NBO** | Occ | Energy (au) | Ionicity (%)[a] | $c_A$[b] | %s | %p | %d | %f | $c_B$[b] | %s | %p | %d | %f |
| **Alpha Spin** | | | | | | | | | | | | | |
| $\mathbf{n_{Pt}}$ | 0.9920 | -0.3655 | | | | | | | | 0 | 0 | 100 | 0 |
| $\mathbf{n_{Pt}}$ | 0.9916 | -0.3649 | | | | | | | | 0 | 0 | 100 | 0 |
| $\mathbf{n_{Pt}}$ | 0.9351 | -0.3703 | | | | | | | | 3 | 0 | 97 | 0 |
| $\mathbf{n_{Th}}$ | 0.9999 | -1.0650 | | | 0 | 99 | 0 | 0 | | | | | |
| $\mathbf{n_{Th}}$ | 0.9998 | -1.3671 | | | 28 | 71 | 0 | 0 | | | | | |
| $\mathbf{n_{Th}}$ | 0.9997 | -1.2617 | | | 27 | 72 | 1 | 0 | | | | | |
| $\mathbf{n_{Th}}$ | 0.9996 | -1.4062 | | | 45 | 53 | 2 | 0 | | | | | |
| $\mathbf{n_C}$ | 0.9860 | -0.6072 | | | | | | | | 75 | 25 | 0 | 0 |
| $\boldsymbol{\pi_{Th\text{-}Pt}}$ | 0.9977 | -0.3945 | 79.97 | 0.316 | 0 | 1 | 74 | 24 | 0.949 | 0 | 0 | 100 | 0 |
| $\boldsymbol{\pi_{Th\text{-}Pt}}$ | 0.9879 | -0.3963 | 82.64 | 0.295 | 0 | 1 | 56 | 43 | 0.956 | 1 | 0 | 99 | 0 |
| $\boldsymbol{\sigma_{Th\text{-}Pt}}$ | 0.9864 | -0.3088 | 39.84 | 0.549 | 75 | 3 | 17 | 5 | 0.836 | 96 | 0 | 4 | 0 |
| $\boldsymbol{\pi_{Th\text{-}C}}$ | 0.9987 | -0.2967 | 38.43 | 0.555 | 0 | 1 | 84 | 14 | 0.832 | 0 | 100 | 0 | 0 |
| $\boldsymbol{\sigma_{Th\text{-}C}}$ | 0.9950 | -0.4273 | 58.98 | 0.453 | 5 | 2 | 73 | 20 | 0.892 | 8 | 92 | 0 | 0 |
| $\boldsymbol{\sigma_{Th\text{-}C}}$ | 0.9898 | -0.5083 | 60.45 | 0.445 | 2 | 1 | 62 | 35 | 0.896 | 18 | 82 | 0 | 0 |
| **Beta Spin** | | | | | | | | | | | | | |
| $\mathbf{n_{Pt}}$ | 0.9920 | -0.3649 | | | | | | | | 0 | 0 | 100 | 0 |
| $\mathbf{n_{Pt}}$ | 0.9907 | -0.3637 | | | | | | | | 0 | 0 | 100 | 0 |
| $\mathbf{n_{Pt}}$ | 0.9292 | -0.3617 | | | | | | | | 5 | 0 | 95 | 0 |
| $\mathbf{n_{Th}}$ | 0.9999 | -1.0591 | | | 0 | 99 | 0 | 0 | | | | | |
| $\mathbf{n_{Th}}$ | 0.9997 | -1.6574 | | | 63 | 37 | 1 | 0 | | | | | |
| $\mathbf{n_{Th}}$ | 0.9958 | -1.0478 | | | 4 | 95 | 1 | 0 | | | | | |
| $\mathbf{n_{Th}}$ | 0.9745 | -1.2930 | | | 34 | 65 | 1 | 0 | | | | | |
| $\boldsymbol{\pi_{Th\text{-}Pt}}$ | 0.9836 | -0.3838 | 77.32 | 0.337 | 9 | 1 | 65 | 25 | 0.942 | 9 | 0 | 91 | 0 |
| $\boldsymbol{\pi_{Th\text{-}Pt}}$ | 0.9977 | -0.3938 | 79.97 | 0.316 | 0 | 1 | 74 | 24 | 0.949 | 0 | 0 | 100 | 0 |
| $\boldsymbol{\sigma_{Th\text{-}Pt}}$ | 0.9745 | -0.3189 | 42.13 | 0.553 | 57 | 3 | 34 | 6 | 0.853 | 86 | 0 | 14 | 0 |
| $\boldsymbol{\pi_{Th\text{-}C}}$ | 0.9987 | -0.2617 | 38.43 | 0.555 | 0 | 1 | 84 | 14 | 0.832 | 0 | 100 | 0 | 0 |
| $\boldsymbol{\sigma_{Th\text{-}C}}$ | 0.9924 | -0.5907 | 77.24 | 0.337 | 14 | 1 | 68 | 16 | 0.941 | 98 | 2 | 0 | 0 |

[a]= $c_B^2 - c_A^2$ [b] Polarization coefficients

The analysis indicates there are seven lone pairs on CThPt. Three are in Pt 5d orbitals, and four are on Th. One Th lone pair is found in a 6p orbital, and three in majority 6p orbitals with 6s mixing for alpha spin. For beta spin, one of the orbitals is majority 6s with 6p mixing. Combining the spins, there is a clearer picture of a σ-type and 2 π-type bonds between Th and Pt. The σ-type bond consists of mixing between the predominantly 7s Th orbital and the predominantly 6s Pt orbital. The π-type bond involves the remaining Pt 5d orbitals bonding with Th 6d/5f orbitals, where the orbital is majority 6d. There is also a σ-type and one π-type bond between Th and C, excluding the Th-C half bond. The σ-type bond consists of a Th 6d/5f orbital with majority 6d and a C sp orbital, and the π-type bond is a Th 6d/5f orbital and C 2p orbital. The alpha and beta Lewis structures of CThPt are found in Figure 4.4. The anion was found to have similar NBO character with the third electron in a Th predominantly 7s orbital (73% s, 14% p, 10% d, 3% f). Its NBO configuration is found in Equation 4.3.

$$(n_{Th})^2(n_{Th})^2(n_{Th})^2(n_{Th})^2(n_C)^2(\sigma_{ThC})^2(\pi_{ThPt})^2(\sigma_{ThC})^1(\sigma_{ThPt})^2(n_{Pt})^2(n_{Pt})^2(n_{Pt})^2(n_{Pt})^2(\pi_{ThC})^2(n_{Th})^1 \quad (4.3)$$

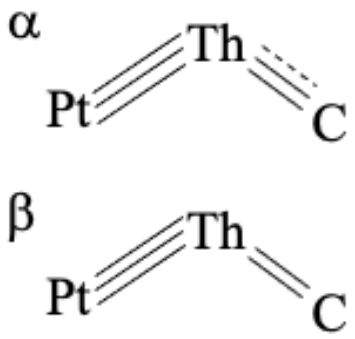


**Figure 4.4 – The Lewis Structures (in α and β spins) for CThPt**

## Conclusions

In this chapter, the geometric and electronic structures of $ThPtC^-$ were determined from the Bowen lab's anion photoelectron spectroscopy data. It was determined that while the vertical electron affinities of ThCPt and CThPt (1.47 eV and 1.49 eV, respectively) are within 1 kcal/mol of experiment (1.50 eV), the bent "insertion" arrangement, C-Th-Pt, has a structure 7.84 kcal/mol lower than the linear "carbonyl" arrangement Th-C-Pt. This is different than what was isolobally expected.[16] The NBO analysis of CThPt, the insertion isomer, shows complex bonding patterns emerging throughout the molecule, with a σ–type and 2 π-type bonds between Th and Pt, while there are 2.5 bonds between Th and C (1.5 σ-type bonds and 1 π-type bond).

# CHAPTER FIVE: ACCURATE AB INITIO CALCULATIONS OF THERMOCHEMICAL PROPERTIES OF ACTINYLS

## Introduction

The most notable family of actinide molecules would be actinide oxides due to their relation to the nuclear fuel cycle, whether they are minor actinides (Np, Am, and Cm) via irradiation or the major players, U and Pu.[1–4] Uranium oxides have been studied extensively.[2,26,27,107–110] One particularly extensive study was done by Infante et al.,[5] where he looked at ionization potentials for actinide (U-Cm) mono and dioxides computationally via CASSCF/CASPT2. There is interest in seeing if higher accuracy methods, like FPD, could provide greater accuracy to these numbers, as well as calculate other thermochemical properties, such as bond dissociation energies and electron affinities.

Small actinide oxides have been studied experimentally in the gas phase.[26,111–113] For instance, Marçalo et al.[26] compiled gas-phase energetics of IPs and BDEs. While this gives a comprehensive list of IPs and BDEs for AnO and $AnO_2$ species (Th-Cm), the experimental uncertainties are rather large, with 2.4 kcal/mol being the smallest for BDEs and as large as 40.6 kcal/mol. The IP experimental uncertainties are tighter, with the smallest being 0.0005 kcal/mol for ThO and as large as 23.06 kcal/mol. Ideally, theoretical work could provide more accurate thermochemical properties and pinpoint where in the large experimental uncertainty these properties fall.

Work has previously been done theoretically to determine the BDEs of $AnO_2^{0/+/2+}$ (An = U, Np, Pu) species.[27] Here nine $AnO_2^{n+}$ (An = U, Np, Pu; n = 0-2) BDEs were determined. However, only four of the composite results (O-$UO^{2+}$, O-NpO, O-$PuO^{2+}$, and O-PuO) agree well,

with experimental findings, that is, fall within experimental uncertainty, even after the experimental value is adjusted to 0 K. This could be due to no correlation recovered for $\Delta E_{SO}$, no $\Delta E_{QED}$ contribution, the basis set chosen, or perhaps an inappropriate system for CCSD(T) to accurately perform.

Finally, as noted in previous chapters, electron affinities of actinide-containing systems are of recent interest.[24,25] The EA of UO was determined to be 1.1407 (7) eV[25] and the EA of $UO_2$ was measured to be 1.159(20) eV[24] or 1.1688(6) eV[25] via photoelectron spectroscopy. Both papers predicted the electron figuration ($7s^25f^1$). $UO_2^-$ was calculated,[24] where scalar relativistic effects were taken into account. CCSD(T) and CASPT2 were used to analyze the molecule. It was concluded the ground electronic state is $^2\Phi_{5/2u}$. $UO^-$ was looked at by Czekner et al.[25] While no calculations were run for $UO^-$, they predicted a ground state configuration of $7s^25f^3$ since it should be isoelectronic to UF.

This chapter seeks to determine highly accurate thermochemical properties (IPs, BDEs, and EAs) of uranium and neptunium oxides via FPD, including the use of correlated methods to obtain $\Delta E_{SO}$, inclusion of $\Delta E_{QED}$, and newer basis sets.

**Computational Methods**

The Feller-Peterson-Dixon (FPD) method has been according to Equation 5.1 to best describe the system at 0 K. Most of these calculations were performed at the CCSD(T) level of theory with the X2C Hamiltonian and aug-cc-pVXZ-DK basis sets for O and cc-pVXZ-X2C for U and Np, with additional diffuse functions added for U when calculating an electron affinity. Core-valence calculations incorporated weighted core-valence basis sets (e.g., cc-pwCVXZ-

X2C) with otherwise the same schema. Triatomic molecules were optimized at the FC-CCSD(T)/VQZ level of theory, while diatomic molecules were optimized at the CCSD(T)/CBS(wCV) level. The optimized geometry was used in calculating the remaining contributions. All but the spin-orbit-related calculations were performed with the MOLPRO quantum chemistry package,[65–67] and the spin-related calculations were performed with DIRAC.[71]

$$E_{FPD} = E_{VQZ} + \Delta E_{CBS} + \Delta E_{CV} + \Delta E_{SO} + \Delta E_{Gaunt} + \Delta E_{QED} + E_{ZPE} \quad (5.1)$$

$E_{VQZ}$ is the base energy at the FC CCSD(T)/cc-pVQZ-X2C level of theory. $\Delta E_{CBS}$ is the difference between the FC-CCSD(T)/cc-pVQZ-X2C energy and the CBS limit determined by extrapolating cc-pVTZ-X2C and cc-pVQZ-X2C results using the formulas described in Chapter 2. $\Delta E_{CV}$ was obtained by extrapolating the CV contribution (difference in a CCSD(T) calculation with and without the outer-core electrons correlated) to the CBS limit using cc-pwCVTZ-X2C and cc-pwCVQZ-X2C basis sets. The outer-core was defined as the 1s orbital for O; and 5s, 5p, and 5d orbitals for U and Np. $\Delta E_{QED}$ was calculated with cc-pwCVTZ-X2C basis sets as described in Ref.69. For triatomic uranium oxides, $E_{ZPE}$ was determined by calculating harmonic frequencies with the cc-pVTZ-X2C basis sets at the CCSD(T) level of theory. Triatomic neptunium oxide ZPEs were calculated in a similar manner but without symmetry due to symmetry breaking. The diatomic molecule ZPEs were calculated from harmonic frequencies and anharmonicity constants calculated at the CCSD(T)/CBS(wCV) level of theory force constants obtained from polynomial fits to near-equilibrium potential energy functions determined by 7 calculated energies distributed about $r_e$.

$\Delta E_{SO}$ was calculated as described in Chapter 2 at the optimized geometry specified above (FC-CCSD(T)/VQZ for dioxides, CCSD(T)/CBS(wCV) for monoxides). Uncontracted aug-cc-

pVDZ (O) and cc-pVDZ-DK3 (U and Np) basis sets were used. For the atoms and molecules, the open-shell definition in the average-of-configuration Dirac Hartree-Fock (AoC-DHF) calculations were specified as shown in Table 5.1. Triatomic uranium molecules could be treated with 4-component CCSD(T), as these were still fairly single determinantal in nature. The remaining molecules had too much multi-reference character, so for all thermochemical properties except for the IPs of $UO_2$, KRCI and MRCI were used instead. All the calculations were carried out on the ground electronic state correlating all the valence electrons except the An 6s (U and Np 6p, 7s, and 5f; O 2s orbitals, and O 2p). A virtual orbital cut-off was chosen based on a well-defined energy gap in the virtual spinors/orbitals (c.f., Table 5.1). $\Delta E_{Gaunt}$ was calculated with the same AoC-DHF parameters as the difference between Dirac-Coulomb-Gaunt and Dirac-Coulomb AoC-DHF calculations with uncontracted aug-cc-pVTZ (O) and cc-pVTZ-DK3 (U) basis sets for uranium oxides, and uncontracted VDZ basis sets for neptunium oxides.

The only other contribution needed is the ionization energy of U, $\Delta E_{IE}$, which is necessary for determining the BDE of UO. Since uranium atom is too multireference for CCSD(T) to be a viable option, UO is calculated by determining the BDE with $U^+$ and O, since the $7s^2 5f^3$ ground state of $U^+$ is more amenable to calculation by CCSD(T). The BDE is then corrected to the ground state of the U atom using the experimental ionization energy 6.19405(6) eV.[114,115]

Finally, in regard to BDEs, most experimental values are determined at 298 K. The calculated FPD BDE values are therefore corrected up to 298 K using spectroscopic constants calculated for these molecules, which will be shown via $\Delta E_{298K}$. For example, the BDE of UO was determined to be 181.4 ± 2.4 kcal/mol at 298.15 K.[23] Using the calculated spectroscopic constants and standard ideal gas partition function expressions,[116] it was determined that the

change in enthalpy from 0 K to 298.15 K is 2.11 kcal/mol, so the modified calculated value is determined to be 182.08 kcal/mol at 298 K, up from 179.96 kcal/mol at 0 K for the BDE of UO.

**Table 5.1 – DIRAC Specifications Involving Open-Shell and Correlation Energy Calculations**

| Molecule | Open-shell [$e^-$/spinor] | Virtual orbital Cut-off (a.u.) | Orbital Character |
|---|---|---|---|
| $UO_2^-$ | 1/0,4 | 12.0 | $5f_\phi$ |
| $UO_2$ | 1/0,4; 1/2,0 | 12.0 | $5f_\Phi$; 7s |
| $UO_2^+$ | 1/0,4 | 12.0 | $5f_\phi$ |
| $UO_2^{2+}$ | - | 12.0 | - |
| $UO^-$ | 3/14 | 12.0 | $5f_{\phi\delta\pi\sigma}$ |
| UO | 4/20 | 12.0 | $5f_{\phi\delta\pi\sigma}7s6d_\delta$ |
| $UO^+$ | 3/20 | 12.0 | $5f_{\phi\delta\pi\sigma}7s6d_\delta$ |
| $UO^{2+}$ | 2/20 | 12.0 | $5f_{\phi\delta\pi\sigma}7s6d_\delta$ |
| $NpO_2$ | 2/0,8; 1/2,0 | 12.0 | $5f_{\phi\delta}$, 7s |
| $NpO_2^+$ | 2/0,8 | 12.0 | $5f_{\phi\delta}$ |
| $NpO_2^{2+}$ | 1/0,4 | 12.0 | $5f_\phi$ |
| NpO | 5/12 | 12.0 | $5f_{\phi\delta\pi}7s$ |
| $NpO^+$ | 4/14 | 12.0 | $5f_{\phi\delta\pi\sigma}$ |
| $NpO^{2+}$ | 3/12 | 12.0 | $5f_{\phi\delta\pi}$ |
| $U^+$ | 3/0,14 | 15.0 | $5f_{\phi\delta\pi\sigma}$ |
| $U^{2+}$ | 4/0,14 | 15.0 | $5f_{\phi\delta\pi\sigma}$ |
| Np | 4/0,14; 1/10,0 | 12.0 | $5f_{\phi\delta\pi\sigma}6d_{\delta\pi\sigma}$ |
| $Np^+$ | 1/2,0; 4/0,14; 1/10,0 | 12.0 | $7s5f_{\phi\delta\pi\sigma}6d_{\delta\pi\sigma}$ |
| $Np^{2+}$ | 5/0,14 | 12.0 | $5f_{\phi\delta\pi\sigma}$ |
| O | 4/6 | - | $2p_{\pi\sigma}$ |

## Results & Discussion

The geometric parameters are provided in Table 5.2. The electronic ground states from this work agree with previous findings.[5,24,25,27] The bond lengths are also in good agreement with previous findings, where there are a few hundredths of Angstroms in fluctuation,[5,24,27] and this work is the first reported bond length for $UO^-$. These structures follow a trend whereas the charge on the species increases, the bond length decreases. This was apparent in the previous literature as well. While the present work on neptunium oxides resulted in similar geometries and

electronic states as in the literature, it was noted by Infante et al.[5] that in general neptunium monoxides, especially $NpO^+$, are highly multi-determinantal. Thus, CCSD(T) cannot adequately describe the ground states of these molecules if that is the case. The Np thermochemical properties were still calculated, however, to showcase the consequences of using a single determinant theory on a multi-determinantal system.

**Table 5.2 – CCSD(T) Equilibrium Geometries Calculated in this Work**

| Molecule | Electronic State | r (Å) |
|---|---|---|
| $UO_2^-$ | $^2\Phi_{5/2u}$ | 1.824 |
| $UO_2$ | $^3\Phi_{2u}$ | 1.794 |
| $UO_2^+$ | $^2\Phi_{5/2u}$ | 1.756 |
| $UO_2^{2+}$ | $^1\Sigma_g^+$ | 1.697 |
| $UO^-$ | $^4I_{9/2}$ | 1.872 |
| UO | $^5I_4$ | 1.839 |
| $UO^+$ | $^4I_{9/2}$ | 1.799 |
| $UO^{2+}$ | $^3H_4$ | 1.726 |
| $NpO_2$ | $^4H_{7/2g}$ | 1.769 |
| $NpO_2^+$ | $^3H_{4g}$ | 1.734 |
| $NpO_2^{2+}$ | $^2\Phi_{5/2u}$ | 1.691 |
| NpO | $^6\Phi_{3/2}$ | 1.829 |
| $NpO^+$ | $^5I_4$ | 1.786 |
| $NpO^{2+}$ | $^4I_{9/2}$ | 1.721 |

*Uranium Oxide Thermochemical Properties*

The IPs and AEAs for uranium oxides are found in Table 5.3. With the absence of any correlation corrections beyond CCSD(T), the current FPD value approach has an expected accuracy of better than 3 kcal/mol (0.13 eV) when the wave function is dominated by the HF determinant. The uranium triatomics had few unpaired electrons, so CCSD(T) could be used to

calculate these IPs. However, the uranium monoxides (and all the neptunium species) had too many open shell electrons, making them too multi-determinantal when SO was included. Hence these species, including the EA of $UO_2$, $\Delta E_{SO}$ was calculated using KRCI/MRCI. It should be noted that the second IPs of $UO_2$ (14.97 eV) and UO (12.91 eV) are probably more accurate than the current experimental values, since the later have relatively large uncertainties, 0.4 eV and 0.6 eV, respectively. The EA of UO is just outside the 3 kcal/mol expected accuracy. All other results are within 0.03 eV at most of the accurate experimental values. As this is well below the FPD targeted accuracy of 0.13 eV, and the uncertainties are tight, these FPD values are in excellent agreement with experiment.

As shown in Table 5.3, $\Delta E_{CBS}$ is almost negligible (0.00-0.01 eV) for the EAs and 1$^{st}$ IPs but contributes roughly 0.04 eV (~ 1 kcal/mol) for the 2$^{nd}$ IPs. $\Delta E_{CV}$ are positive, with the 2$^{nd}$ IP contributions being significantly larger than the EA and 1$^{st}$ IP values. $\Delta E_{SO}$ are roughly 1-2 kcal/mol in magnitude, except in the case of the 2$^{nd}$ IPs, which are at least twice as large. This is likely due to the 2$^{nd}$ IP removing a 5f electron rather than a 7s electron, as is the case for the other thermochemical properties. $\Delta E_{Gaunt}$ are similarly sized across the board, except for the 2$^{nd}$ IP of UO (0.04 kcal/mol). $\Delta E_{QED}$ are all similar in magnitude, being at most roughly 0.5 kcal/mol.